



Proteomic Analysis of the Hydrogen and Carbon Monoxide Metabolism of *Methanothermobacter marburgensis*

Martijn Diender^{1*}, Ricardo Pereira¹, Hans J. C. T. Wessels², Alfons J. M. Stams^{1,3} and Diana Z. Sousa¹

¹ Laboratory of Microbiology, Wageningen University, Wageningen, Netherlands, ² Department of Laboratory Medicine, Radboud University Medical Center, Nijmegen, Netherlands, ³ Centre of Biological Engineering, University of Minho, Braga, Portugal

Hydrogenotrophic methanogenic archaea are efficient H₂ utilizers, but only a few are known to be able to utilize CO. *Methanothermobacter thermoautotrophicus* is one of the hydrogenotrophic methanogens able to grow on CO, albeit about 100 times slower than on H₂ + CO₂. In this study, we show that the hydrogenotrophic methanogen *Methanothermobacter marburgensis*, is able to perform methanogenic growth on H₂/CO₂/CO and on CO as a sole substrate. To gain further insight in its carboxydrotrophic metabolism, the proteome of *M. marburgensis*, grown on H₂/CO₂ and H₂/CO₂/CO, was analyzed. Cultures grown with H₂/CO₂/CO showed relative higher abundance of enzymes involved in the reductive acetyl-CoA pathway and proteins involved in redox metabolism. The data suggest that the strong reducing capacity of CO negatively affects hydrogenotrophic methanogenesis, making growth on CO as a sole substrate difficult for this type of methanogens. *M. marburgensis* appears to partly deal with this by up-regulating co-factor regenerating reactions and activating additional pathways allowing for formation of other products, like acetate.

Keywords: syngas, methanogenesis, CODH, reductive acetyl-CoA pathway, *Methanothermobacter thermoautotrophicus*

OPEN ACCESS

Edited by:

Regina-Michaela Wittich,
Spanish National Research Council
(CSIC), Spain

Reviewed by:

James F. Holden,
University of Massachusetts
Amherst, USA
Tapan Kumar Adhya,
KIIT University, India

*Correspondence:

Martijn Diender
martijn.diender@wur.nl

Specialty section:

This article was submitted to
Microbiotechnology, Ecotoxicology
and Bioremediation,
a section of the journal
Frontiers in Microbiology

Received: 30 March 2016

Accepted: 22 June 2016

Published: 04 July 2016

Citation:

Diender M, Pereira R, Wessels HJCT, Stams AJM and Sousa DZ (2016) Proteomic Analysis of the Hydrogen and Carbon Monoxide Metabolism of *Methanothermobacter marburgensis*. *Front. Microbiol.* 7:1049. doi: 10.3389/fmicb.2016.01049

INTRODUCTION

Methanogenesis from hydrogen, acetate, methanol, or methanethiols is a relatively well-studied process (Thauer et al., 2008). In 1931, CO was shown to potentially act as a substrate for methanogens in mixed cultures (Fischer et al., 1931), but knowledge of carboxydrotrophic methanogenesis is still rather limited. Gaining insight in CO-driven methanogenesis is not only of interest from a fundamental point of view, but also from an applied scope. The rapid development of syngas technology makes it cheaper to convert any carbon rich source into a gaseous mixture, consisting mainly of CO, H₂, and CO₂ (syngas). Syngas-driven carboxydrotrophic methanogenesis can be considered as an alternative to biogas production via anaerobic digestion. About 10–25% of the biomass consists of lignin, which is difficult to degrade biologically and can even prevent degradation of easily degradable biopolymers such as hemicellulose (Daniell et al., 2012; Jönsson and Martín, 2016). Additionally, biomass-derived biogas contains a fraction of 25–45% CO₂ (De Mes et al., 2003) and needs to be subsequently upgraded to bio-methane before injection in the gas grid is possible. Via the syngas route a higher substrate conversion yield can be achieved, and by increasing the H₂ content of the gas substrate a CO₂-free end product can be obtained in one process step.

Carbon monoxide appears to be a difficult substrate for methanogens, and only three methanogens have been shown to utilize it for growth: *Methanothermobacter thermoautotrophicus* (Daniels et al., 1977), *Methanosarcina barkeri* (O'Brien et al., 1984; Bott et al., 1986), and *Methanosarcina acetivorans* (Rother and Metcalf, 2004). Carboxydrotrophic growth of *M. thermoautotrophicus* is possible with CO as a sole carbon source up to pressures of 50 kPa. Doubling times reported for CO-grown *M. thermoautotrophicus* are about 200 h, which is about a 100 times slower than with H₂/CO₂ (Daniels et al., 1977). *M. barkeri* was observed to utilize 100 kPa CO, but also at a relatively slow doubling time (about 65 h) compared to growth on other substrates (O'Brien et al., 1984). *Methanosarcina acetivorans* can withstand higher CO partial pressures (>150 kPa) and grows on CO with a doubling time of about 20 h. However, it shifts its methanogenic metabolism toward formation of acetate and formate with increasing CO pressures (Rother and Metcalf, 2004). Detailed research has been performed on the CO metabolism of *M. acetivorans* (Rother and Metcalf, 2004; Lessner et al., 2006; Rother et al., 2007; Matschiavelli et al., 2012), providing more insight in the enzymes involved in carboxydrotrophic metabolism of this acetoclastic methanogen. Currently, *M. thermoautotrophicus* is the only hydrogenotrophic methanogen known that can grow on CO as a substrate, and there is limited knowledge on the carboxydrotrophic metabolism of hydrogenotrophic methanogens in general. Carboxydrotrophic methanogenesis is expected to be operated in a similar way as hydrogenotrophic metabolism (Daniels et al., 1977; Diender et al., 2015). Electrons derived from the oxidation of CO or H₂ are used to reduce CO₂ to methyl-tetrahydromethanopterin (methyl-H₄MPT). This key-intermediate can subsequently be converted into either methane, for energy generation, or assimilated via acetyl-CoA, for biomass production.

In this study, we aimed to assess the CO-metabolism of *Methanothermobacter marburgensis*. *M. marburgensis* has a highly similar CODH sequence to that of *M. thermoautotrophicus* (93% identity). Additionally, it was shown that the methyl-coenzyme M reductase (MCR) of *M. marburgensis* was activated 15 times faster by CO than by H₂ (Zhou et al., 2013). Here we show that *M. marburgensis* can grow methanogenically on CO and we assessed its carboxydrotrophic metabolism via physiological analysis and proteomics. Additionally, we evaluated the limitations of this type of metabolism, which is theorized to be related to hydrogenase inhibition or redox-stress (Diender et al., 2015).

MATERIALS AND METHODS

Strains and Cultivation

Strains *M. thermoautotrophicus* (DSM 1053) and *M. marburgensis* (DSM 2133) were obtained from the German Collection of Microorganisms and Cell Cultures (DSMZ; Braunschweig, Germany). Strains were initially cultivated at 65°C on recommended *Methanobacterium* medium (DSM-119) using anaerobic cultivation procedures. After growth was confirmed,

the strains were adapted to growth in a carbonate-phosphate buffered medium with the following composition: 0.4 g/l KH₂PO₄, 0.53 g/l K₂HPO₄ * 2 H₂O, 0.3 g/l NH₄Cl, 0.3 g/l NaCl, 0.1 g/l MgCl₂ * 6 H₂O, 0.5 g/l yeast extract and 0.5 mg/l resazurin. Medium was supplemented, per liter, with 61.8 μg H₃BO₃, 61.25 μg MnCl₂, 943.5 μg FeCl₂, 64.5 μg CoCl₂, 12.86 μg NiCl₂, 67.7 μg ZnCl₂, 13.35 μg CuCl₂, 17.3 μg Na₂SeO₃, 29.4 μg Na₂WO₄, and 20.5 μg Na₂MoO₄. Medium was prepared, boiled and cooled under a continuous nitrogen flow. Bottles (120 ml total volume, 50 ml liquid) were filled with medium and instantly capped with rubber stopper and aluminum cap. The gas phase was exchanged with either 80:20 N₂/CO₂ or 80:20 H₂/CO₂, resulting in a final pressure of 170 kPa. When necessary, the headspace was further fine-tuned by addition of CO, keeping final pressure at 170 kPa. The bottles were autoclaved and stored at room temperature till further use. Before inoculation medium was supplied with the following volumes of stock solutions: 1% of 11 g/l CaCl₂ * 2 H₂O, 1% of a vitamin solution containing per liter: biotin 20 mg, nicotinamide 200 mg, *p*-aminobenzoic acid 100 mg, thiamin 200 mg, panthotenic acid 100 mg, pyridoxamine 500 mg, cyanocobalamin 100 mg, riboflavin 100 mg. The medium was reduced by introducing a 5% volume of a stock solution containing 4.8 g/l Na₂S * *x* H₂O (*x* = 7 – 9) and 80 g/l NaHCO₃. Unless stated otherwise, bottles were inoculated with an exponentially growing culture in a 1:50 ratio (v/v).

Analytical Procedures

Headspace composition was determined by gas chromatography using a GC-2014 (Shimadzu, Kyoto, Japan) equipped with a thermal conductivity detector. H₂, CH₄, and CO were measured with a Molsieve 13X column, 2 m long and an inner diameter of 3 mm. Argon was used as carrier gas at a flow rate of 50 ml/min. Injector, column and detector temperatures were set to 80, 60, and 130°C, respectively. CO₂ was measured separately in a CP Poraplot column of 25 m × 0.53 mm, with a stationary phase film thickness of 20 μm, employing helium as carrier gas at a flow rate of 15 ml/min. Injector, column and detector temperatures were set to 60, 34, and 130°C, respectively. The detection limits for H₂, CO, CO₂, and CH₄ were 20, 250, 20, and 80 Pa, respectively.

Liquid phase composition was analyzed via high pressure liquid chromatography equipped with a MetaCarb 67H column (Agilent Technologies, Santa Clara, CA, USA). The column was operated at a temperature of 45°C with a flow rate of 0.8 ml/min using 0.01 N H₂SO₄ as eluent. Detection of acetate was done using an RI and UV detector. Concentrations of 0.5 mM could be accurately determined and lower levels are referred to as trace amounts.

Cell Free Extract Preparation and Measuring CO-Oxidation Activity

Cells of *M. marburgensis* were grown on either 80:20 H₂/CO₂ or 60:20:20 H₂/CO₂/CO. Biological triplicates were prepared for each condition. Cells were harvested at end log-phase in an anaerobic tent, where the broth was centrifuged at 13000 × g for

10 min. Supernatant was discarded and the pellets were dissolved in 1 ml 50 mM Tris-HCl, pH 8. Cells were disrupted using a VC-40 sonicator (Sonics materials, Newtown, CT, USA) using five cycles of 30 s sonication, at a power input of 20 W, followed by 30 s rest at 0°C. Cell free extract (CFE) was put in 5 ml glass vials and capped with rubber stoppers inside the anaerobic tent. Subsequently, the headspace of these vials was exchanged to 1.5 bar N₂ to remove traces of H₂.

CO-oxidation activity of the CFE was determined as follows: glass cuvettes (2 ml total volume) were closed with a rubber stopper and flushed three times by using 5 ml N₂ or CO. Subsequently, 1 ml assay buffer (50 mM MOPS, pH 7, 20 mM methyl viologen (MV) and 2 mM DTT) was added to the cuvette and reduced with 1 µl of 100 mM dithionite. The cuvette was put into a pre-heated U-2010 spectrophotometer (Hitachi, Tokyo, Japan) and was left to heat up to 60°C. Absorption of MV was measured at 578 nm. The initial extinction was set to a value between 0.2 and 0.6. After obtaining a stable baseline, 50 or 25 µl CFE was added to the cuvette, initiating the reaction. Each separate biological sample was assessed for CO-oxidizing activity and endogenous activity (using N₂ instead of CO). The initial activity of CO-oxidation after CFE addition was taken, and corrected for the initial slope of the endogenous activity. In order to confirm that CO was the electron donor, cuvettes were prepared with N₂ headspace and CFE was added. After seizure of endogenous activity 0.3 ml CO was added to the sample as initiation trigger. Each biological sample was at least analyzed in duplicate using either 50 or 25 µl CFE. An extinction coefficient 9.7 mM⁻¹ cm⁻¹ (Bonam and Ludden, 1987) was used for MV at 578 nm. Protein concentration in the CFE was determined by using Roti-Nanoquant protein quantitation assay (CarlRoth, Karlsruhe, Germany), according to manufacturer instructions.

Sample Preparation for Proteomics

Duplicate cultures of *M. marburgensis* grown in two conditions, 80:20 H₂/CO₂ and 60:20:20 H₂/CO₂/CO, were harvested in late exponential phase by centrifugation (cultivation was performed in 1 l anaerobic bottles containing 500 ml medium). Prior to centrifugation cultures were quickly cooled down on ice and kept at 4°C for 30 min to decrease cell activity. Cell pellets were resuspended in TE buffer (10 mM Tris-Cl, pH 7.5; 1 mM EDTA) containing 1 mM phenylmethanesulfonyl fluoride, and passed through a French pressure cell operated at 138 MPa. Proteins were stabilized by addition of 8 M of urea in a proportion of 1:1 and samples were concentrated using a 3.5 kDa MWCO filter. Final protein concentration in samples obtained for LC-MS/MS analysis were assessed using Qubit® Protein Assay Kit in a Qubit® 2.0 Fluorometer (Life technologies). Samples were subjected to in-solution tryptic digestion as described elsewhere (Wessels et al., 2010).

LC-MS/MS Data Acquisition

Protein samples obtained from the two sets of biological duplicates were analyzed in duplicate using C18 reversed phase liquid chromatography with online tandem mass spectrometry (LC-MS/MS). Measurements were performed using a nanoflow

ultra-high pressure liquid chromatograph (nano-Advance; Bruker Daltonics) coupled online to an orthogonal quadrupole time-of-flight mass spectrometer (maXis 4G ETD, otofControl v3.4 build 14; Bruker Daltonics) via an axial desolvation vacuum assisted electrospray ionization source (Captive sprayer; Bruker Daltonics). Five microliters of tryptic digest were loaded onto the trapping column (Acclaim PepMap 100, 75 µm × 2 cm, nanoViper, 3 µm 100Å C18 particles; Thermo Scientific) using 0.1% FA at a flow rate of 9000 nl/min for 3 min at room temperature. Next, peptides were separated on a C18 reversed phase 15 cm length × 75 µm internal diameter analytical column (Acclaim PepMap RSLC, 75 µm × 15 cm, nanoViper, 2 µm 100Å C18 particles; Thermo scientific) at 40°C using a linear gradient of 3–35% ACN 0.1% FA in 120 min at a flow rate of 600 nl/min. The mass spectrometer was operated in positive ion mode and was tuned for optimal ion transmission in the range of m/z 300–1400. Electrospray ionization conditions were 3 l/min 180°C N₂ drying gas, 1400 V capillary voltage and 0.4 Bar N₂ for gas phase supercharging (nanobooster) using acetonitrile as dopant. Parameters for optimal ion transmission were funnel RF: 400 Vpp, multipole RF: 400 Vpp, quadrupole ion energy: 5.0 eV, quadrupole low mass: 300 m/z, collision cell energy: 9.0 eV, collision cell RF: 3500 Vpp, ion cooler transfer time: 64 µs, ion cooler RF: 250 Vpp, pre-pulse storage: 22 µs. Data dependent acquisition of MS/MS spectra (AutoMSn) was performed using a 3 s duty cycle at 2 Hz acquisition rate for full MS spectra and a variable number of MS/MS experiments at precursor intensity scaled spectra rate (3 Hz MS/MS spectra rate at 2000 counts, 20 Hz MS/MS spectra rate @ 100.000 counts). Precursor ions within the range of 400–1400 m/z with charge state $z = 2+$ or higher (preferred charge state range of $z = 2+$ to $z = 4+$) were selected for MS/MS analysis with active exclusion enabled (excluded after one spectrum, released after 0.5 min, reconsidered precursor if current intensity/previous intensity ≥ 4 , smart exclusion disabled). Spectra were saved as line spectra only and were calculated from profile spectra as the sum of intensities across a mass spectral peak (five counts absolute threshold, peak summation width seven points).

Proteomics Analysis

Protein identification and relative quantitation was performed using the MaxQuant software (v.1.5.0.0; Cox and Mann, 2008) using the build-in Andromeda database search algorithm. Extracted MS/MS spectra were searched against the SWISS-PROT *M. marburgensis* protein sequence database. Amino acid sequences of known contaminant proteins (e.g., skin and hair proteins, Trypsin, LysC) were added to the database. The following settings were used for peptide and protein identification: carbamidomethyl (Cys) as fixed modification, oxidation (Met), and deamidation (NQ) as variable modifications, predefined MS and MS/MS settings for TOF instruments, minimal peptide length six amino acids and a maximum allowed false discovery rate of 1% at both the peptide and protein level. Label free quantitation (LFQ) was performed with the match between runs and re-quantify options using at least 2 razor + unique peptides. Retention

time alignment was performed with a time alignment window of 20 min and a retention time match window of 0.5 min. Label-free quantitation (LFQ) values were used for subsequent data analysis. Proteins quantified in at least three out of four measurements for either growth condition were analyzed by student's *t*-tests to identify differentially expressed proteins with $p < 0.05$. The mass spectrometry proteomics data have been deposited to the ProteomeXchange Consortium via the PRIDE (Vizcaino et al., 2016) partner repository with the dataset identifier PXD003661.

RESULTS

Carboxydrotrophic Growth of *M. thermoautotrophicus* and *M. marburgensis*

Both, *M. thermoautotrophicus* and *M. marburgensis* were capable of growing methanogenically on H₂/CO₂/CO or CO as a sole substrate. When assessing the production profiles on H₂/CO₂/CO, it appears that both strains co-utilize H₂ and CO (Figure 1). For both strains H₂ utilization becomes slower with exposure to higher CO pressures. The maximal H₂ consumption rate of *M. marburgensis* dropped from 1.3 to 0.43 mmol/l_{liquid}/h when increasing the CO pressure from 0 to 70 kPa. Similarly *M. thermoautotrophicus* decreased its maximal H₂ consumption rate from 0.55 to 0.19 mmol/l_{liquid}/h when increasing the CO pressure from 0 to 70 kPa. *M. marburgensis* could be grown on CO as a sole substrate up to 50 kPa (data not shown), which is similar to the value found for *M. thermoautotrophicus* (Daniels et al., 1977).

M. marburgensis appears to utilize carbon monoxide more easily as it depletes 34 kPa CO within 120 h, while *M. thermoautotrophicus* uses this substrate significantly slower (Figure 1). This suggests that *M. marburgensis* can be better adapted to carboxydrotrophic growth than *M. thermoautotrophicus*. It was attempted to adapt both strains to cultivation on purely CO by repeatedly transferring them in presence of solely CO as electron donor. The initial lag phase of *M. marburgensis* growing solely on 34 kPa CO was ~500 h, but in the two subsequent transfers the lag phase for CO conversion decreased to ~100 h (Figure 2). CO consumption and methane production rates between these transfers did not change significantly (Figure 2). Cultures transferred back to H₂/CO₂ quickly lost this adaptation to CO and showed again a longer lag phase when incubated with CO alone. Nevertheless, a re-adaptation of these cultures to CO was possible. Growth of *M. thermoautotrophicus* on H₂/CO₂/CO or CO as the sole substrate could not be improved via subsequent transfers, nor could the lag phase be decreased. Due to this inefficient growth of *M. thermoautotrophicus* in presence of CO it was decided to perform further analysis and proteomics solely with *M. marburgensis*.

In all cultures of *M. marburgensis* growing on CO as a sole substrate, H₂ is observed to accumulate in the headspace before the onset of methanogenesis (Figure 2). Upon initiation

of carboxydrotrophic methanogenesis, H₂ is co-utilized. At the end of cultivation, not all the CO is converted to methane as approximately 1 mol methane is formed per 6 mol CO consumed (Figure 2), suggesting formation of other products. Acetate formation was observed in incubations of *M. marburgensis* grown in presence of CO, which ranged from 2 to 4 mM at the end of cultivation.

Assessing the *M. marburgensis* CO oxidizing activity in the CFE of H₂/CO₂/CO grown cells resulted in a specific MV reducing activity of $2.74 \pm 0.3 \mu\text{mol MV min}^{-1} \text{mg protein}^{-1}$ after correction for endogenous activity. H₂/CO₂ grown cells showed a specific MV reducing activity of $2.06 \pm 0.13 \mu\text{mol MV min}^{-1} \text{mg protein}^{-1}$ after correction for endogenous activity, which is about 1.3 times lower than in the condition with CO. Additionally, the CFE of H₂/CO₂ grown cells showed no endogenous activity, while cells grown on H₂/CO₂/CO showed an average initial endogenous activity of $0.6 \mu\text{mol MV min}^{-1} \text{mg protein}^{-1}$. This endogenous activity decayed over time, completely seizing after ~150 s. Addition of CO, after seizure of endogenous activity, resulted again in reduction of MV in all samples.

Comparative Proteomics of *M. marburgensis*

Comparative proteomic analysis was performed on *M. marburgensis* incubated with 80:20 H₂/CO₂ or 60:20:20 H₂/CO₂/CO. In the proteomics analysis 5845 peptides from 831 non-redundant proteins were identified [false discovery rate (FDR) $\leq 1\%$, average absolute mass error: $1.14 \pm 1.76 \text{ ppm}$] of which 590 proteins were quantified using at least two razor + unique peptides in ≥ 3 measurements of either growth condition. Both the technical and biological reproducibility was very good based on median LFQ standard deviations of 6.9 and 18.4%, respectively. In total, 203 proteins were found to be differentially abundant between the two growth conditions (student's *t*-test $p < 0.05$, median LFQ standard deviation: 14.8%).

All the proteins required for hydrogenotrophic methanogenesis and the reductive acetyl-CoA pathway could be detected in both the H₂/CO₂- and H₂/CO₂/CO-grown cultures (Figure 3). In presence of CO, several subunits of carbon monoxide dehydrogenase (CODH) and acetyl-CoA synthase (ACS) were more abundant. Several enzymes in the methyl-branch of the acetyl-CoA pathway were found to be increased in abundance in the presence of CO (Table 1): mainly the formylmethanofuran dehydrogenase, methyl-coenzyme M reductase-I and the F420 dependent methylene-H₄MPT dehydrogenase. Additionally, a higher abundance of the subunit H of the tetrahydromethanopterin S-methyltransferase was detected with CO as substrate. Other subunits of this complex were not significantly overproduced, and levels of subunit B and G were even lowered. Also, a predicted acetyl-CoA synthetase, theorized to be involved in acetate metabolism, was found to be more abundant.

Polyferredoxin, belonging to the energy conserving hydrogenase (EcH), was more abundant in the presence of

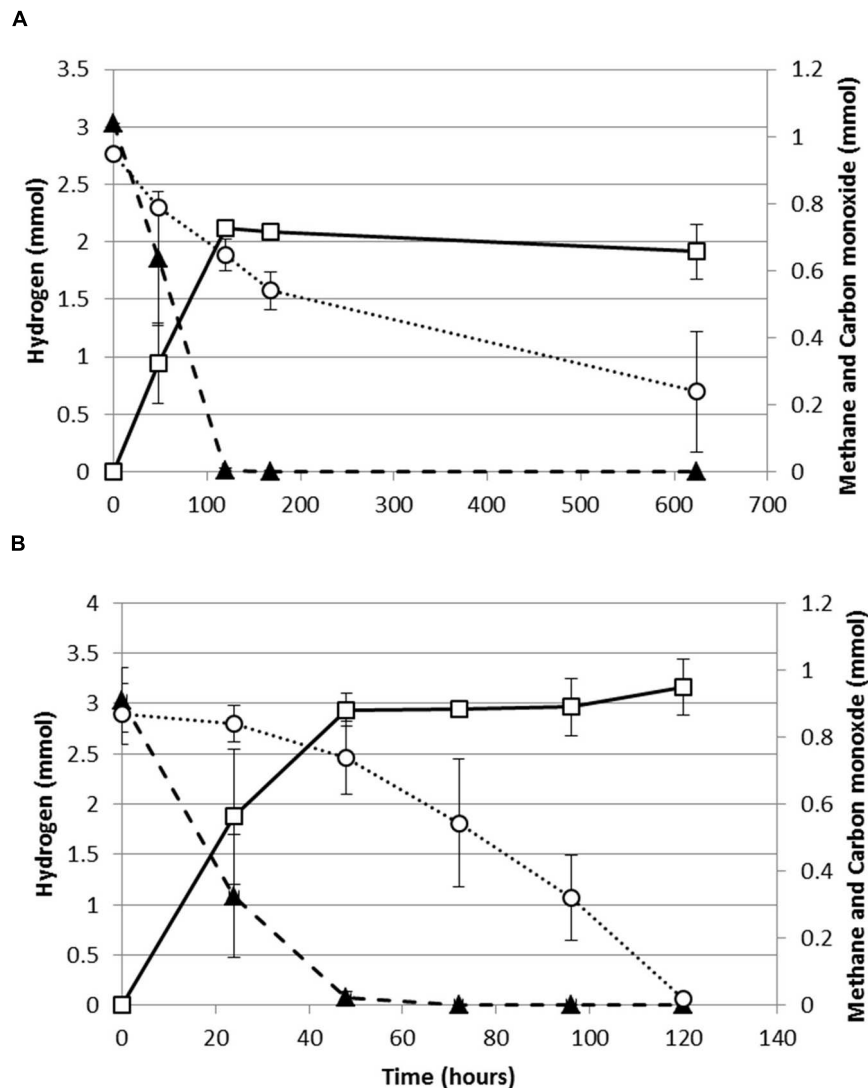


FIGURE 1 | Production profile of hydrogenotrophic methanogens growing on H₂/CO₂/CO. (A) Production profile of *M. thermoautotrophicus*. **(B)** Production profile of *M. marburgensis*. Hydrogen: solid black triangles, Methane: open black squares, Carbon monoxide: open black circles. Gas is represented as total amount of mmol present in the bottle headspace. Error bars display maximal and minimal amounts over duplicate experiments.

CO, but other subunits of this Ech were not clearly differentially present. Other hydrogenase related proteins, such as the HypE protein, involved in hydrogenase maturation, and subunits of the F420-reducing hydrogenase were also found to be more abundant in cultures grown with CO in the headspace. In presence of CO, several proteins related to redox stress were found in higher numbers: F420 oxidase, superoxide dismutase, superoxide reductase, and F390 synthetase (**Supplementary Table S1**). In addition to redox stress proteins, a predicted universal stress protein was found to be more abundant. Also a decrease in 30S and 50S ribosomal proteins was observed in presence of CO. Tuning down of ribosomal RNA and ribosomal proteins, is often observed as a response to different types of stress in *Escherichia coli* (Wagner, 1994), but also in other microorganisms this is observed (Abee and Wouters, 1999; van

de Guchte et al., 2002). The decrease in ribosomal proteins in *M. marburgensis* in presence of CO could thus potentially be an additional indication of stress.

DISCUSSION

When growing on hydrogen, hydrogenotrophic methanogens generate methyl-H₄MPT required in the final part of methanogenesis (Thauer et al., 2008). In addition, they can assimilate acetyl-CoA from methyl-H₄MPT for biosynthetic purposes, by using the ACS. This requires CODH activity to reduce CO₂ to CO, which is subsequently condensed with methyl-H₄MPT and CoA-SH to form acetyl-CoA. For methanogens, the CODH complex is in almost all

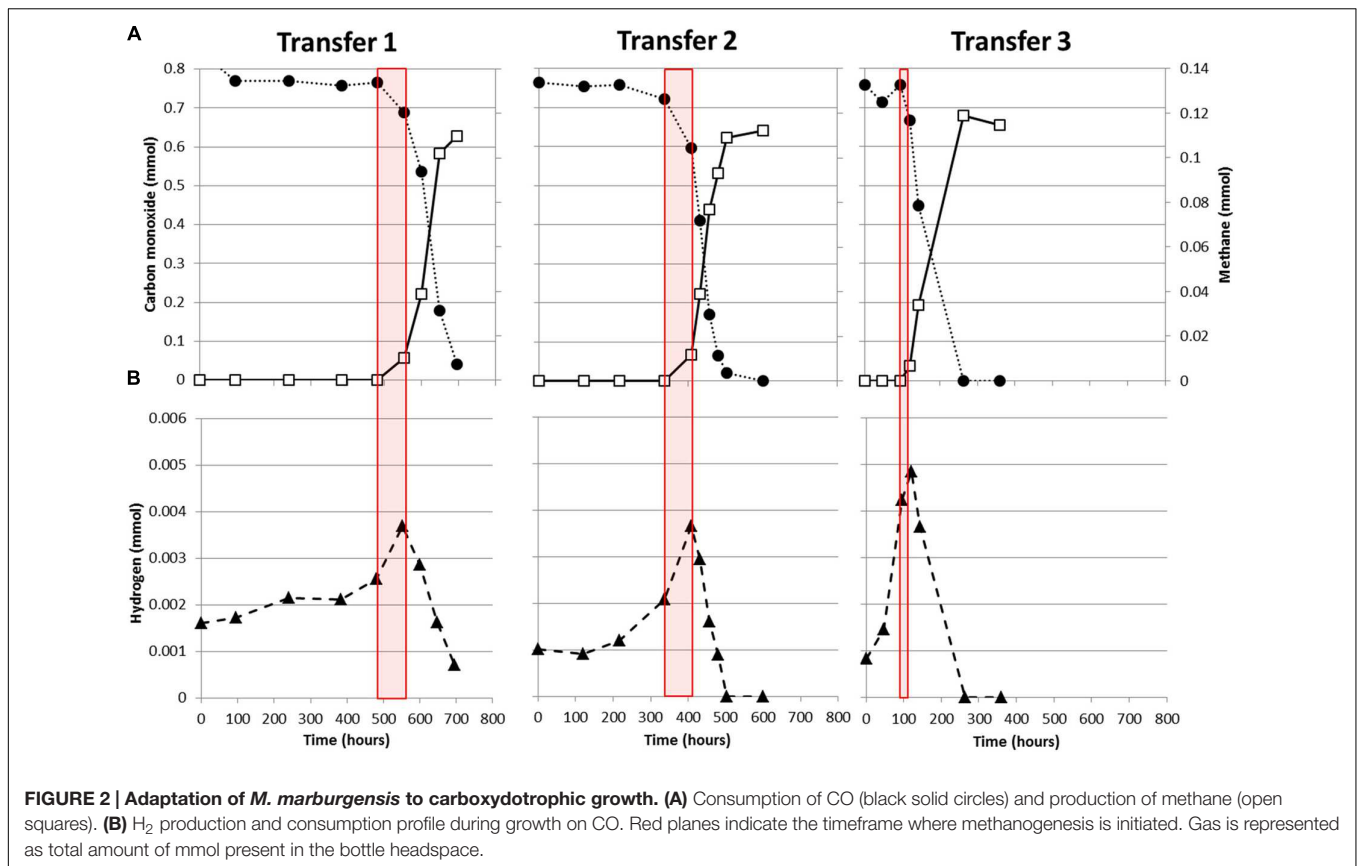


FIGURE 2 | Adaptation of *M. marburgensis* to carboxydrotrophic growth. (A) Consumption of CO (black solid circles) and production of methane (open squares). **(B)** H₂ production and consumption profile during growth on CO. Red planes indicate the timeframe where methanogenesis is initiated. Gas is represented as total amount of mmol present in the bottle headspace.

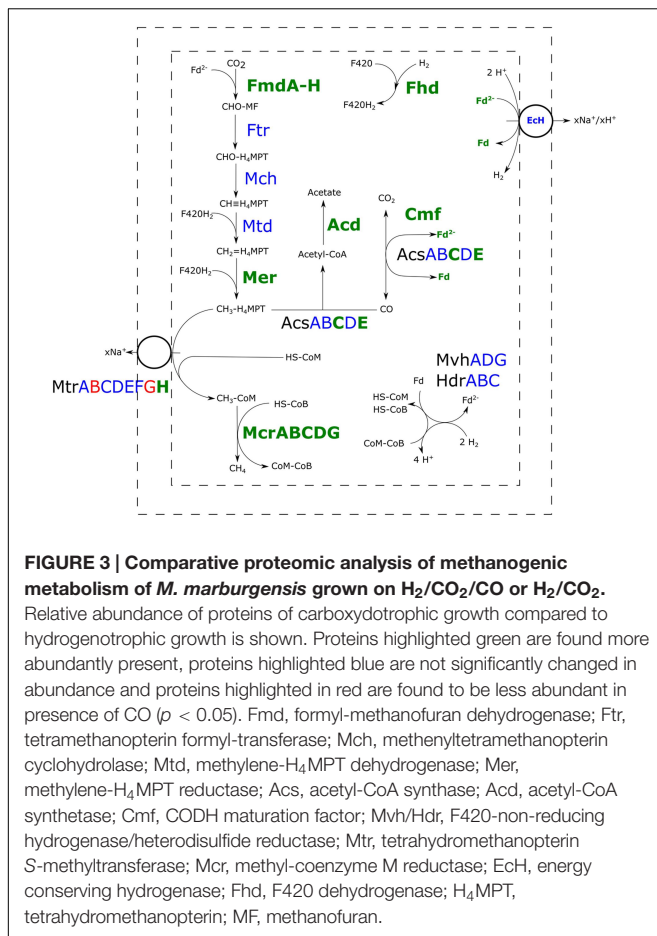
cases associated with an ACS complex (Techtmann et al., 2012), suggesting it mainly plays a role in the assimilatory metabolism.

CODH/ACS Related Metabolism

The slight, but significant, increase in CO-oxidation activity observed in the CFE of H₂/CO₂/CO grown cultures compared to the CFE of H₂/CO₂ grown cells suggests that more CO-oxidizing enzymes are present. This is in accordance with the higher abundance of several CODH/ACS related proteins when *M. marburgensis* is grown in the presence of CO: the epsilon and gamma subunit of the main complex, the CODH maturation protein and a CODH related ferredoxin. Two CODH-related operons can be found in the genome of *M. marburgensis* (*cdh1* and *cdh2*; Liesegang et al., 2010). The *cdh2* operon codes for all the five subunits of a CODH/ACS, a CODH-like maturation factor and a CODH-related ferredoxin. Detection of the complete CODH/ACS complex under both of the tested conditions suggests that it is at least involved in assimilatory metabolism. Higher abundance of several CODH subunits, the CODH maturation factor and the CODH-related ferredoxin in the H₂/CO₂/CO condition could indicate that the complex is also involved in CO-oxidation, allowing transfer of electrons to other co-factors/proteins. Such an observation is also made in *M. acetivorans* of which the genome contains two CODH/ACS operons (*cdh1* and *cdh2*). Higher abundance of these CODH/ACS complexes was observed during proteomic analysis comparing

CO-grown to acetate- or methanol-grown cultures. This suggests an important role for the CODH/ACS complex in CO-oxidation (Lessner et al., 2006; Rother et al., 2007). It has been shown later on that both Cdh isoforms of *M. acetivorans* are functional CODH/ACS complexes and that one isoform is sufficient for catabolic and anabolic functions (Matschiavelli et al., 2012). It is therefore likely that the CODH/ACS complex of *M. marburgensis* plays a main role in CO-oxidation.

The *cdh1* operon of *M. marburgensis* contains the sequence of one pseudo annotated CODH alpha subunit and a sequence coding for a HycB-like, ferredoxin-related, protein. The presence of the HycB gene next to the CODH sequence could indicate that this protein is involved in CO-oxidation. However, its function remains unclear as this protein is not detected in the H₂/CO₂ nor the H₂/CO₂/CO condition. The genome of *M. acetivorans* contains three other CODH sequences in addition to the two CODH/ACS operons: two monofunctional CODH related genes (*cooS1F* and *cooS2*) and one operon containing solely the alpha subunit of the CODH/ACS complex (*cdhA3*). Knockout studies showed that the two monofunctional CODHs are not essential for CO utilization, as CO was still utilized as a substrate in the knockout strains (Rother et al., 2007). These monofunctional CODHs were observed to have a function at elevated CO pressures as detoxification mechanism. The CdhA3 protein is suggested to play a role in CO sensing and is apparently not directly involved in CO oxidation (Matschiavelli et al., 2012). The Cdh1 of *M. marburgensis* was not detected in the conditions



tested here, and thus no conclusions can be drawn on its function. However, as the CO concentrations used in this study are relatively low, it is possible this protein is involved in CO-detoxification at higher CO pressures, similar to the observation in *M. acetivorans*. However, a different role or non-functionality of this protein cannot be ruled out.

Methyl-Branch Related Proteins

In addition to CODH/ACS related proteins, several enzymes involved in the methyl-branch of the reductive acetyl-CoA pathway were more abundant in cultures grown on H₂/CO₂/CO. In particular, formylmethanofuran dehydrogenase, acting in the formation of formylmethanofuran from CO₂, and the F420-dependent methylene-H₄MPT dehydrogenase, involved in generation of methyl-H₄MPT from methylene-H₄MPT, are significantly more abundant in incubations with CO (Table 1, Figure 3). Both proteins play a role in re-oxidation of co-factors, and their higher abundance might assist in countering the redox pressure of CO. Other proteins involved in the methyl-branch stay similar in abundance compared to incubations with H₂/CO₂ (Figure 3).

The higher abundance of several enzymes in the methyl-branch in H₂/CO₂/CO-grown *M. marburgensis* is expected to result in an increased flow through the pathway and thus

requires up-regulation of subsequent pathways. This might explain the ‘switching-on’ of the acetate formation pathway and the increased production of enzymes involved in the final steps of methanogenesis (Figure 3). The observed acetate formation by *M. marburgensis* in presence of CO is supported by the finding of higher abundance of a predicted acetyl-coenzyme A synthetase (E.C. 6.2.1.1), theorized to be involved in acetate production and consumption. Proteomics data of *M. marburgensis* grown on H₂/CO₂/CO shows higher abundance of all subunits of methyl-coenzyme M reductase. Additionally, the H-subunit of tetrahydromethanopterin methyl-transferase is found to be more abundant. Studies on the H-subunit in *M. thermoautotrophicus* shows it catalyses the conversion of cob(I)alamin with CH₃-H₄MPT to methylcob(III)alamin, but lacks conversion activity of methylcob(III)alamin to methyl-CoM in absence of the rest of the complex (Hippler and Thauer, 1999). Other subunits of this complex are unchanged or even lowered in abundance in presence of CO (Figure 3). The membrane associated nature of this protein complex might have hindered accurate quantification, making it difficult to assess the relative abundance of the different subunits between the two conditions. This hinders the assessment of the role of the complex as a whole in the carboxydrotrophic methanogenic metabolism of *M. marburgensis*.

Comparing the proteomics results obtained here with results reported for *M. acetivorans* is difficult as the native aceticlastic metabolism of *M. acetivorans* is different from the hydrogenotrophic metabolism of *M. marburgensis*. *M. acetivorans* cannot be grown on hydrogen and comparative proteomic studies with CO have been performed using acetate and methanol as alternative substrates (Lessner et al., 2006; Rother et al., 2007). A detailed comparison between the carboxydrotrophic metabolism of *M. acetivorans* and *M. marburgensis* would therefore not be accurate.

Limitations in Hydrogenotrophic Carboxydrotrophic Methanogenic Metabolism

Carbon monoxide affects metalloproteins by interacting with their active-centers via back-bonding (Jeoung et al., 2014). Hydrogenases are considered CO-sensitive enzymes and H₂ metabolism of several microbial strains is inhibited by CO (Daniels et al., 1977; Genthner and Bryant, 1982; Bertsch and Müller, 2015). However, [Ni-Fe]-hydrogenases are considered more robust and more resistant to CO-inhibition (Adams, 1990; De Lacey et al., 2007). Hydrogenases involved in methanogenesis are in general [Ni-Fe]-hydrogenases, except for the iron-only hydrogenase present in *M. thermoautotrophicus*, replacing the methylene-H₄MPT reductase in nickel deprived conditions (Afting et al., 1998, 2000). Higher CO-pressures seem to inhibit the metabolism of both *M. thermoautotrophicus* and *M. marburgensis*, as can be seen from the slowing down in H₂ consumption rate. However, the ability of both strains to co-utilize H₂ and CO suggests hydrogenase inhibition is not the only mechanism of toxicity in these hydrogenotrophic methanogens.

Carbon monoxide has a low redox-potential ($E^{\circ} = -520$ mV), which can be seen as a major difficulty for the

TABLE 1 | Highlighted set of more abundant proteins of *M. marburgensis* grown on H₂/CO₂/CO vs. H₂/CO₂.

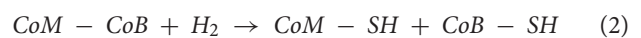
Protein	Relative abundance (H ₂ /CO ₂ /CO vs. H ₂ /CO ₂)
Methanogenesis related proteins	
Tungsten formylmethanofuran dehydrogenase (subunit A)	2.13
Tungsten formylmethanofuran dehydrogenase (subunit B)	3.16
Tungsten formylmethanofuran dehydrogenase (subunit C)	1.7
Tungsten formylmethanofuran dehydrogenase (subunit D)	2.36
Tungsten Formylmethanofuran dehydrogenase (subunit F)	1.48
Tungsten formylmethanofuran dehydrogenase (subunit G)	2.4
F420-dependent methylene-H4MPT dehydrogenase	1.68
Methyl-coenzyme M reductase component A2-like protein	2.06
Methyl-coenzyme M reductase I subunit alpha	1.97
Methyl-coenzyme M reductase I subunit beta	1.63
Methyl-coenzyme M reductase I subunit gamma	1.8
Methyl-coenzyme M reductase I operon protein D	9.63
Methyl-coenzyme M reductase I operon protein C	unique to H ₂ /CO ₂ /CO
Tetrahydromethanopterin S-methyltransferase subunit H	1.83
CODH/ACS related proteins	
Acetyl-CoA synthase, subunit gamma	1.76
Acetyl-CoA synthase, subunit epsilon	4.62
Carbon monoxide dehydrogenase, iron sulfur subunit	3.48
CO dehydrogenase maturation factor	unique to H ₂ /CO ₂ /CO
Acetate related genes	
Predicted acetyl-coenzyme A synthetase	3.11

A cutoff value of $p < 0.05$ was used to assess if proteins were more abundantly present. The complete proteomics dataset can be found in **Supplementary Table S1**.

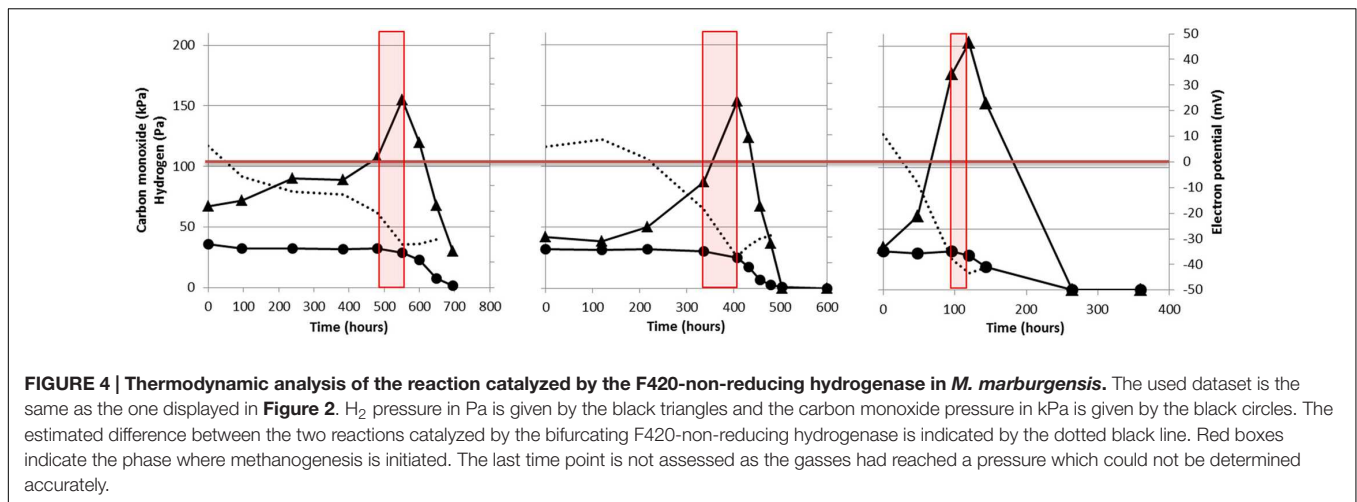
methanogens. Generation of ferredoxin by hydrogenotrophic methanogens is in general done via reverse proton transport via the EcH or a bifurcation reaction performed by a F420-non-reducing hydrogenase (Buckel and Thauer, 2013). The low redox potential of CO does, however, allow for direct reduction of ferredoxin via CODH, making reduced ferredoxin more accessible in the cell. This lowers the Fd_{ox}/Fd_{red} ratio in the cell, lowering the electron potential of the ferredoxin couple. Judging from proteomics data, several redox response systems are activated. However, many of these, such as the superoxide dismutase and F420-oxidase, are normally a response to oxidized compounds (e.g., oxygen), which is the opposite of the more reduced environment created by CO. It might be that these genes respond to redox stress in general or are regulated by universal stress proteins. Additionally, the F390-synthetase, involved in redox sensing was found to be more abundant. In *M. thermoautotrophicus*, this system was found to react on changes in redox potential, regulating the expression of MCR-I, F420-dependant MDH, and the F420-reducing hydrogenase (Vermeij et al., 1997). The CFE of H₂/CO₂/CO grown cells showed more endogenous activity when compared to H₂/CO₂ grown cells. This could indicate more reducing equivalents are present in the cells grown in presence of CO. The overall increase in abundance of proteins involved in redox stress and co-factor regeneration, and the higher endogenous reducing activity suggest that *M. marburgensis* cells exposed to CO are subjected to changes in redox balance.

When grown solely on CO, *M. marburgensis* shows production of H₂ from the moment incubation is started

(Figure 2). Methanogenesis is not started instantly, and CO appears to be solely used for H₂ production. Methanogenesis initiates only after H₂ has accumulated in the headspace (Figures 2 and 4) and, from that point on, quickly co-utilizing H₂ and CO. These data suggest that a minimal amount of H₂ is required to operate the carboxydrotrophic methanogenic metabolism. We theorize this is related to the properties of the bifurcating F420-non-reducing hydrogenase required to regenerate CoM-SH and CoB-SH. Feasibility of the overall bifurcating reaction was estimated by calculating the potential difference between the two separate reactions catalyzed (Eqs 1 and 2). The following assumptions were made during calculation: (I) pH is assumed to be 7 and temperature 338 K, (II) the ferredoxin couple is assumed to have a standard electron potential of -500 mV under physiological conditions (Thauer et al., 2008), but is assumed to approach the electron potential of the CO/CO₂ couple at the respective partial pressures (assessed via Nernst equation). Similarly the electron potential of H₂ is assumed to be similar to its partial pressure, (III) the CoM-CoB couple is assumed to have an electron potential of -140 mV, and (IV) the bifurcation reaction is considered feasible if the sum in potential of reaction 1 and 2 has a negative value.



$$E^{0'} = - 274 \text{ mV}$$



H₂ has to drive the reduction of both CoM–CoB and ferredoxin in the reaction catalyzed by the F420-non-reducing hydrogenase. However, as the electron potential of ferredoxin is expected to be lowered in presence of CO, and H₂ is almost absent in the cultures, the overall reaction becomes less exergonic. When assessing the difference between the two separate reactions, it is observed that the overall reaction is not favored under the starting conditions of incubation (Figure 4, dotted lines). Under these conditions the CoM–SH and CoB–SH cannot be replenished, potentially blocking methanogenesis. As more H₂ is generated, via the Ech complex, the reaction becomes more favorable, eventually allowing to start methanogenesis (Figure 4). Inhibition of hydrogenases or an irreversible reduced state of the cell at higher CO pressures could prevent H₂ production and consumption, preventing the methanogenic metabolism from starting. The proposed limitation of the F420-non-reducing hydrogenase might explain why hydrogenotrophic methanogens as *M. marburgensis* and *M. thermoautotrophicus* can only utilize CO as a sole substrate up to 50 kPa, whereas *M. barkeri* and *M. acetivorans*, which do not employ a bifurcating F420-non-reducing hydrogenase (Thauer et al., 2008), can perform carboxydrotrophic growth using > 100 kPa and > 150 kPa CO, respectively. The CO metabolism of hydrogenotrophic methanogens is thus potentially limited by their F420-non-reducing hydrogenase, and this would explain the observation that their efficiency of carboxydrotrophic growth is strongly connected to the availability of hydrogen.

CONCLUSION

The hydrogenotrophic methanogen *M. marburgensis*, was found to grow methanogenically on H₂/CO₂/CO or CO alone. CO could be used as a sole substrate up to 50 kPa and its consumption was stimulated in the presence of hydrogen. Proteomic analysis indicates higher abundance of CODH/ACS related proteins and enzymes of the methyl-branch in presence of CO. Most of the abundant proteins in cultures grown in the presence of CO are involved in redox reactions, potentially required to

counter the strong reducing capacity of CO. Additionally, the pathway toward acetate production was found up-regulated, which explains formation of small amounts of acetate as an end-product in presence of CO. The ability to utilize H₂ in the presence of CO suggests that hydrogenase inhibition is not the main mechanism of toxicity in hydrogenotrophic methanogens. The requirement of small amounts of hydrogen, before methanogenesis with CO could start, suggests that this is an essential intermediate in the methanogenic metabolism. The F420-non-reducing bifurcating hydrogenase is a likely candidate for CO inhibition as low H₂ pressures potentially can cause this reaction to become unfavorable, blocking the methanogenic metabolism.

AUTHOR CONTRIBUTIONS

MD: Experimental work, data analysis, drafting and writing manuscript. RP: Experimental work and data analysis. HW: Proteomics and data analysis. AS: Experimental design and critical revision of the manuscript. DS: Experimental design, data analysis, and writing the manuscript.

ACKNOWLEDGMENTS

Research of AS is supported by an ERC grant (project 323009) and a Gravitation grant (project 024.002.002) of the Netherlands Ministry of Education, Culture and Science and the Netherlands Science Foundation (NWO).

SUPPLEMENTARY MATERIAL

The Supplementary Material for this article can be found online at: <http://journal.frontiersin.org/article/10.3389/fmicb.2016.01049>

TABLE S1 | Comparative proteomic analysis of H₂/CO₂ vs. H₂/CO₂/CO grown cells of *Methanothermobacter marburgensis*.

REFERENCES

- Abee, T., and Wouters, J. A. (1999). Microbial stress response in minimal processing. *Int. J. Food Microbiol.* 50, 65–91. doi: 10.1016/S0168-1605(99)00078-1
- Adams, M. W. (1990). The structure and mechanism of iron-hydrogenases. *Biochim. Biophys. Acta* 1020, 115–145. doi: 10.1016/0005-2728(90)90044-5
- Afting, C., Hochheimer, A., and Thauer, R. (1998). Function of H₂-forming methylenetetrahydromethanopterin dehydrogenase from *Methanobacterium thermoautotrophicum* in coenzyme F₄₂₀ reduction with H₂. *Arch. Microbiol.* 169, 206–210. doi: 10.1007/s002030050562
- Afting, C., Kremmer, E., Brucker, C., Hochheimer, A., and Thauer, R. K. (2000). Regulation of the synthesis of H₂-forming methylenetetrahydromethanopterin dehydrogenase (Hmd) and of HmdII and HmdIII in *Methanothermobacter marburgensis*. *Arch. Microbiol.* 174, 225–232. doi: 10.1007/s00203000197
- Bertsch, J., and Müller, V. (2015). CO metabolism in the acetogen *Acetobacterium woodii*. *Appl. Environ. Microbiol.* 81, 5949–5956. doi: 10.1128/AEM.01772-15
- Bonam, D., and Ludden, P. (1987). Purification and characterization of carbon monoxide dehydrogenase, a nickel, zinc, iron-sulfur protein, from *Rhodospirillum rubrum*. *J. Biol. Chem.* 262, 2980–2987.
- Bott, M., Eikmanns, B., and Thauer, R. K. (1986). Coupling of carbon monoxide oxidation to CO₂ and H₂ with the phosphorylation of ADP in acetate-grown *Methanosarcina barkeri*. *Eur. J. Biochem.* 159, 393–398. doi: 10.1111/j.1432-1033.1986.tb09881.x
- Buckel, W., and Thauer, R. K. (2013). Energy conservation via electron bifurcating ferredoxin reduction and proton/Na⁺ translocating ferredoxin oxidation. *Biochim. Biophys. Acta* 1827, 94–113. doi: 10.1016/j.bbabi.2012.07.002
- Cox, J., and Mann, M. (2008). MaxQuant enables high peptide identification rates, individualized ppb-range mass accuracies and proteome-wide protein quantification. *Nat. Biotechnol.* 26, 1367–1372. doi: 10.1038/nbt.1511
- Daniell, J., Köpke, M., and Simpson, S. (2012). Commercial biomass syngas fermentation. *Energies* 5, 5372–5417. doi: 10.3390/en5125372
- Daniels, L., Fuchs, G., Thauer, R., and Zeikus, J. (1977). Carbon monoxide oxidation by methanogenic bacteria. *J. Bacteriol.* 132, 118–126.
- De Lacey, A. L., Fernandez, V. M., Rousset, M., and Cammack, R. (2007). Activation and inactivation of hydrogenase function and the catalytic cycle: spectroelectrochemical studies. *Chem. Rev.* 107, 4304–4330. doi: 10.1021/cr0501947
- De Mes, T., Stams, A., Reith, J., and Zeeman, G. (2003). “Methane production by anaerobic digestion of wastewater and solid wastes,” in *Biomethane and Biohydrogen. Status and Perspectives of Biological Methane and Hydrogen Production*, eds J. H. Reith, R. H. Wijffels, and H. Barten (Petten: Dutch Biological Hydrogen Foundation), 58–102.
- Diender, M., Stams, A. J., and Sousa, D. Z. (2015). Pathways and bioenergetics of anaerobic carbon monoxide fermentation. *Front. Microbiol.* 6:1275. doi: 10.3389/fmicb.2015.01275
- Fischer, F., Lieske, R., and Winzer, K. (1931). Die umsetzungen des kohlenoxyds. *Biochem. Z* 236, 247–267.
- Genthner, B. S., and Bryant, M. (1982). Growth of *Eubacterium limosum* with carbon monoxide as the energy source. *Appl. Environ. Microbiol.* 43, 70–74.
- Hippler, B., and Thauer, R. K. (1999). The energy conserving methyltetrahydromethanopterin: coenzyme M methyltransferase complex from methanogenic archaea: function of the subunit MtrH. *FEBS Lett.* 449, 165–168. doi: 10.1016/S0014-5793(99)00429-9
- Jeoung, J.-H., Fessler, J., Goetzl, S., and Dobbek, H. (2014). “Carbon monoxide. toxic gas and fuel for anaerobes and aerobes: carbon monoxide dehydrogenases,” in *The Metal-Driven Biogeochemistry of Gaseous Compounds in the Environment*, eds P. M. H. Kroneck and M. E. Sosa Torres (Dordrecht: Springer), 37–69.
- Jönsson, L. J., and Martín, C. (2016). Pretreatment of lignocellulose: formation of inhibitory by-products and strategies for minimizing their effects. *Bioresour. Technol.* 199, 103–112. doi: 10.1016/j.biortech.2015.10.009
- Lessner, D. J., Li, L., Li, Q., Rejtar, T., Andreev, V. P., Reichlen, M., et al. (2006). An unconventional pathway for reduction of CO₂ to methane in CO-grown *Methanosarcina acetivorans* revealed by proteomics. *Proc. Natl. Acad. Sci. U.S.A.* 103, 17921–17926. doi: 10.1073/pnas.0608833103
- Liesegang, H., Kaster, A.-K., Wiezer, A., Goenrich, M., Wollherr, A., Seedorf, H., et al. (2010). Complete genome sequence of *Methanothermobacter marburgensis*, a methanoarchaeon model organism. *J. Bacteriol.* 192, 5850–5851. doi: 10.1128/JB.00844-10
- Matschiavelli, N., Oelgeschläger, E., Cocchiario, B., Finke, J., and Rother, M. (2012). Function and regulation of isoforms of carbon monoxide dehydrogenase/acetyl coenzyme A synthase in *Methanosarcina acetivorans*. *J. Bacteriol.* 194, 5377–5387. doi: 10.1128/JB.00881-12
- O'Brien, J. M., Wolkin, R., Moench, T., Morgan, J., and Zeikus, J. (1984). Association of hydrogen metabolism with unitrophic or mixotrophic growth of *Methanosarcina barkeri* on carbon monoxide. *J. Bacteriol.* 158, 373–375.
- Rother, M., and Metcalf, W. W. (2004). Anaerobic growth of *Methanosarcina acetivorans* C2A on carbon monoxide: an unusual way of life for a methanogenic archaeon. *Proc. Natl. Acad. Sci. U.S.A.* 101, 16929–16934. doi: 10.1073/pnas.0407486101
- Rother, M., Oelgeschläger, E., and Metcalf, W. W. (2007). Genetic and proteomic analyses of CO utilization by *Methanosarcina acetivorans*. *Arch. Microbiol.* 188, 463–472. doi: 10.1007/s00203-007-0266-1
- Teichtmann, S. M., Lebedinsky, A. V., Colman, A. S., Sokolova, T. G., Woyke, T., Goodwin, L., et al. (2012). Evidence for horizontal gene transfer of an anaerobic carbon monoxide dehydrogenases. *Front. Microbiol.* 3:132. doi: 10.3389/fmicb.2012.00132
- Thauer, R. K., Kaster, A.-K., Seedorf, H., Buckel, W., and Hedderich, R. (2008). Methanogenic archaea: ecologically relevant differences in energy conservation. *Nat. Rev. Microbiol.* 6, 579–591. doi: 10.1038/nrmicro1931
- van de Guchte, M., Serror, P., Chervaux, C., Smokvina, T., Ehrlich, S. D., and Maguin, E. (2002). Stress responses in lactic acid bacteria. *Antonie Van Leeuwenhoek* 82, 187–216. doi: 10.1023/A:1020631532202
- Vermeij, P., Pennings, J., Maassen, S. M., Keltjens, J. T., and Vogels, G. D. (1997). Cellular levels of factor 390 and methanogenic enzymes during growth of *Methanobacterium thermoautotrophicum* deltaH. *J. Bacteriol.* 179, 6640–6648.
- Vizcaino, J. A., Csordas, A., Del-Toro, N., Dianes, J. A., Griss, J., Lavidas, I., et al. (2016). 2016 update of the PRIDE database and its related tools. *Nucleic Acids Res.* 44, D447–D456. doi: 10.1093/nar/gkv1145
- Wagner, R. (1994). The regulation of ribosomal RNA synthesis and bacterial cell growth. *Arch. Microbiol.* 161, 100–109. doi: 10.1007/BF00276469
- Wessels, H., Gloerich, J., Van Der Biezen, E., Jetten, M., and Kartal, B. (2010). Liquid chromatography-mass spectrometry-based proteomics of *Nitrosomonas*. *Methods Enzymol.* 486, 465–482. doi: 10.1016/B978-0-12-381294-0.00021-3
- Zhou, Y., Dorchak, A. E., and Ragsdale, S. W. (2013). In vivo activation of methyl-coenzyme M reductase by carbon monoxide. *Front. Microbiol.* 4:69. doi: 10.3389/fmicb.2013.00069

Conflict of Interest Statement: The authors declare that the research was conducted in the absence of any commercial or financial relationships that could be construed as a potential conflict of interest.

Copyright © 2016 Diender, Pereira, Wessels, Stams and Sousa. This is an open-access article distributed under the terms of the Creative Commons Attribution License (CC BY). The use, distribution or reproduction in other forums is permitted, provided the original author(s) or licensor are credited and that the original publication in this journal is cited, in accordance with accepted academic practice. No use, distribution or reproduction is permitted which does not comply with these terms.